The increasing role of quantification in clinical nuclear cardiology: The Emory approach

Ernest V. Garcia, PhD, Tracy L. Faber, PhD, C. David Cooke, MSEE, Russell D. Folks, BS, Ji Chen, PhD, and Cesar Santana, MD, PhD

Single photon emission computed tomography (SPECT) myocardial perfusion imaging has attained widespread clinical acceptance as a standard of care for patients with known or suspected coronary artery disease. A significant contribution to this success has been the use of computer techniques to provide objective quantitative assessment in interpreting these studies. We have implemented the Emory Cardiac Toolbox (ECTb) as a pipeline to distribute the software tools that we and others have researched, developed, and validated to be clinically useful so that diagnosticians everywhere can benefit from our work. Our experience has demonstrated that integration of all software tools in a common platform is the optimal approach to promote both accuracy and efficiency. Important attributes of the ECTb approach are (1) our extensive number of normal perfusion databases for SPECT and positron emission tomography (PET) studies, each created with at least 150 patients; (2) our use of Fourier analysis of regional thickening to ensure proper temporal resolution and to allow accurate measurement of left ventricular function and dyssynchrony; (3) our development of PET tools to quantify myocardial hibernation and viability; (4) our development of 3-dimensional displays and the use of these displays as a platform for image fusion of perfusion and computed tomography angiography; and (5) the use of expert systems for decision support. ECTb is an important tool for extracting quantitative parameters from all types of cardiac radionuclide distributions. ECTb should continue to play an important role in establishing cardiac SPECT and PET for flow, function, metabolism, and innervation clinical applications. (J Nucl Cardiol 2007;14:420-32.)

Single photon emission computed tomography (SPECT) myocardial perfusion imaging (MPI) has attained widespread clinical acceptance as a standard of care for patients with known or suspected coronary artery disease (CAD). Evidence of this widespread acceptance is the 10 million patients who were imaged with this procedure in the United States in 2005. A significant contribution to this success has been the use of computer techniques to provide objective quantitative assessment in interpreting these studies. Beyond objective assessment, these computer techniques have been major promoters of standardizing acquisition, processing, display, and analysis protocols. This standardization in turn promotes widespread utilization and quality criteria, important for the success of any modality. Finally, these software techniques provide an efficient platform to perform the previously mentioned functions, so their applications are realistic in the busy and demanding clinical environment. The rest of this article reviews the contributions and tools made by the team from Emory University (Atlanta, Ga) that are part of the Emory Cardiac Toolbox (ECTb).

From Emory University School of Medicine, Atlanta, Ga.
Reprint requests: Ernest V. Garcia, PhD, Emory University Hospital, Room E163, 1364 Clifton Rd, NE, Atlanta, GA 30322; *ernest.garcia@emory.org*.
1071-3581/$32.00

doi:10.1016/j.nuclcard.2007.06.009

ECTB PHILOSOPHY

Our primary goal as a research team is to stay at the leading edge of scientific discovery to diagnose heart disease. We have implemented ECTb as a pipeline to distribute the software tools that we and others have researched, developed, and validated to be clinically useful so that diagnosticians everywhere can benefit from our work. We use a high-level scientific language (IDL) to shorten the time between concept and general distribution, and this frees our scientists to devote most of their time to research and less to programming. We place great emphasis on characterizing the accuracy of our techniques through a validation process that establishes the effectiveness of the software tool (how it will work in the real clinical setting) rather than the efficacy (how it works under ideal conditions). We understand that for diagnosticians to use these quantitative tools, our

software has to be easy to use (automatic) and promote both processing and interpretation efficiency. In our latest implementation of ECTb all studies can be remotely accessed through the use of personal computers with our software or even with any browser on any personal computer that has Internet access (Syntermed Live [Syntermed, Inc, Atlanta, Ga]). If ECTb can save 2 minutes per interpretation in a laboratory that images 30 patients per day, the physician can go home 1 hour earlier. Or better yet, the physician can go home or away from the office and interpret the studies from anywhere.

INTEGRATION

Our experience has demonstrated that integration of all software tools in a common platform is the optimal approach to promote both accuracy and efficiency. Accuracy is promoted because in the common platform, all functions are synergistic. For example, all automatic processing is performed before displaying the tomographic oblique slices for visual interpretation. Because the algorithm has already detected the apex and the base of the rest and stress MPI studies, the software automatically aligns the rest to the stress study. Because the left ventricular (LV) count distribution has already been extracted, ECTb knows the maximal count pixel in the LV myocardium and automatically normalizes the display to that pixel, not to external hot gut uptake, for example. Another example is how we use the multiple gated frames to calculate a more accurate measure of LV mass and then use that mass to determine the mass at jeopardy from the perfusion distribution. We also use the concept of the Active Viewbox mode to generate, in a single display, all of the integrated information required by a diagnostician to make an interpretation (Figure 1). Integration for us also means that a reporting program (Nuclear Report Professional [NRP], Syntermed, Inc) can be launched from ECTb with a single click of the mouse; this brings into the report all of the quantitative parameters deemed useful to include for a specific institution.

QUANTIFICATION OF MYOCARDIAL PERFUSION

Polar Map Representation

For representation of the patient's LV myocardial perfusion distribution and for identifying hypoperfused segments, we use the polar map approach first reported by Garcia et al.[1] In this approach the 3-dimensional (3D) maximal LV count distribution is synthesized onto a single 2-dimensional polar map, where the count distribution at the base of the left ventricle corresponds to the intensity at the periphery of the map and the counts at the apex to the center of the polar map. For detecting hypoperfusion, we use a database quantification approach in which a patient's 3D LV myocardial perfusion tracer uptake is compared with a statistically determined lower limit of normal.[1-3] The rationale is that the program emulates the visual interpretation of experts by establishing both the mean normal distribution (with the corresponding regional SD) and the regional abnormality criteria in terms of how many SDs from the mean normal distribution best separate normal from hypoperfused segments.

The extent of hypoperfusion is shown by a blackout or extent polar map. On this map, the normalized counts of LV segments that fall below the lower limit of normal are deemed to be hypoperfused and are highlighted in black on the polar map. The actual extent of the abnormality is calculated from the 3D distribution rather than from the distorted polar representation. This extent is expressed as either percent or actual mass of the left ventricle hypoperfused. The severity of the hypoperfusion is displayed via an SD or defect severity map. This is done by color-coding the number of SDs below the mean, where white represents the most normal region (those segments that are no more than 1 SD below the mean) and black represents the most abnormal regions (over 7 SDs below the normal mean). To measure the severity of hypoperfusion, we use the total severity score reported by DePuey et al,[4] where the score is given by the total number of SDs below the mean for the entire extent of the abnormality. This score takes into account both the extent and severity of the abnormality.

For quantifying the degree of reversibility in a resting study compared with stress-induced hypoperfusion, we use the method we innovated and that was reported by Klein et al.[5] In this approach a reversibility polar map distribution is calculated by normalizing the same region in the resting distribution to the most normal (5×5–voxel) region in the stress distribution. Once normalized, the stress distribution is subtracted from the resting distribution, and what remains are the areas of improved perfusion at rest or the reversibility map. This approach has been validated in a multicenter trial.[6]

For quantifying viability, we use the extensively validated method of Gibbons et al.[7] This approach is applied to the resting perfusion distribution exclusively. The rationale of this method is that viable myocardial segments exhibit uptake of the perfusion tracer at rest whereas nonviable segments do not. The algorithm searches for the maximal counts in the entire LV myocardial distribution and identifies as nonviable those myocardial segments that fall below a percentage of this maximal value, usually 60% for technetium 99m perfusion agents.

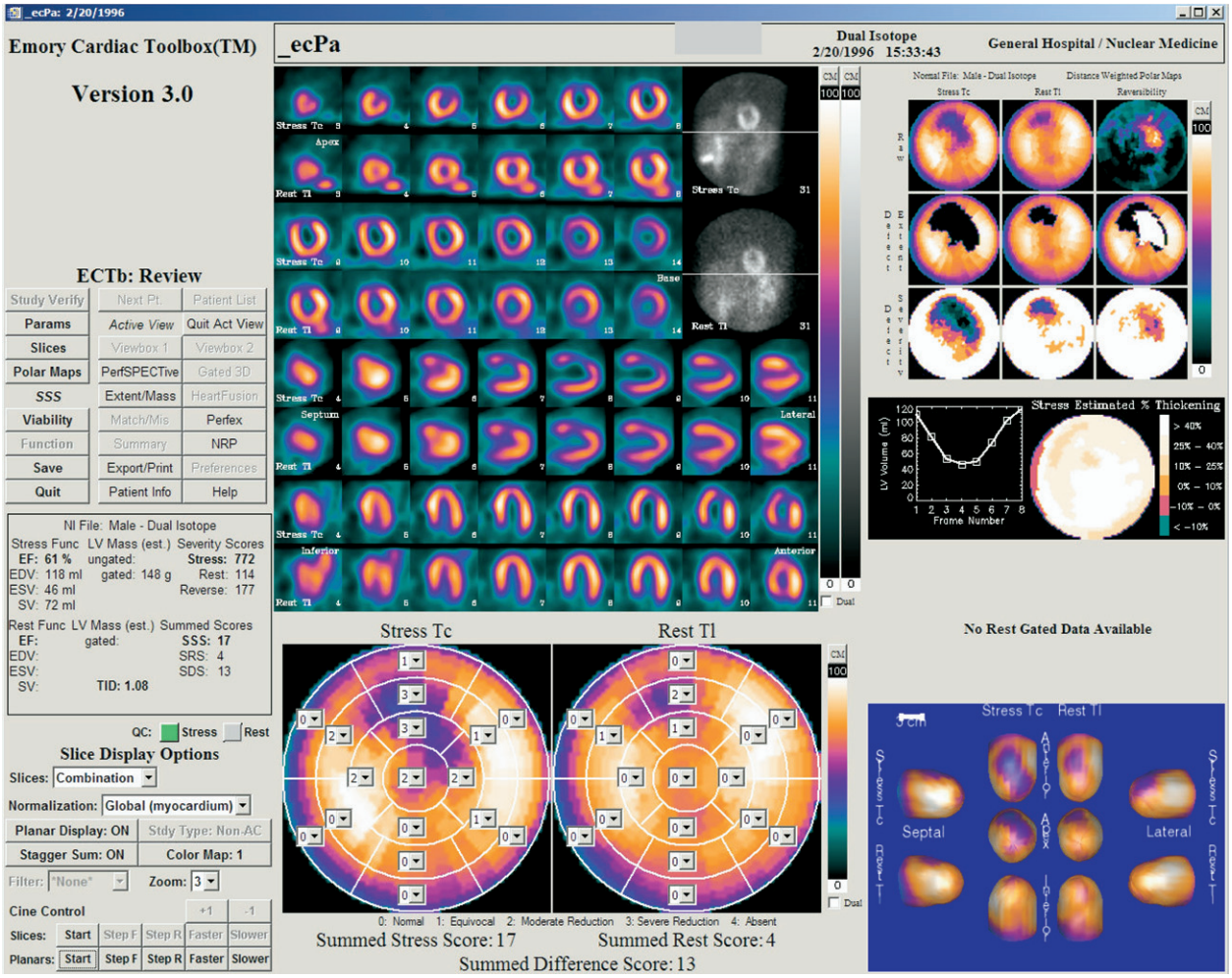

Figure 1. Active Viewbox ECTb display of a patient with a reversible anterior wall stress-induced perfusion defect. The active comprehensive display integrates (1) planar projections, (2) oblique slices, (3) polar maps including normal database comparison, (4) 3D displays, (5) 17-segment summed score polar maps, (6) LV volume/time curve, and (7) regional thickening map. The quantitative measurements reported in the *middle left panel* should be noted. Active display refers to the ability of the operator to control the viewed displays. For example, the planar images are rotated, the tomographic slices may be animated and filtered, the summed scores may be modified, and so on.

Clinically Validated Normal Databases

For generation of normal databases and abnormality criteria, we use the approach of Van Train et al.[8] This approach does not assume that the regional normalized count distribution is a normal (Gaussian) distribution. The reason for not assuming a normal distribution is the realization that the normalization of the 3D LV count distribution to 100% for the hottest myocardial segment places an upper bound in the distribution and distorts the statistics. For example, in normal thallium 201 distributions the hottest wall is always the lateral wall. Because all normal patient distributions are then set to 100% around the same segment, the SD is artificially small.

For generation of each normal database, we use 3 populations: (1) a normal group of usually 30 patients with a low likelihood of CAD determined independently of the MPI study, (2) a criteria group of usually 60 patients selected because they exhibit a spectrum of perfusion abnormalities, and (3) a prospective validation group, preferably from multiple centers, of usually 60 patients who have undergone coronary arteriography as a gold standard. Thus we use a mixture of 150 normal and abnormal patients to generate one database. If the database is for an attenuation-corrected study, then there are no gender differences such as in attenuation-corrected SPECT[9] or positron emission tomography (PET) studies

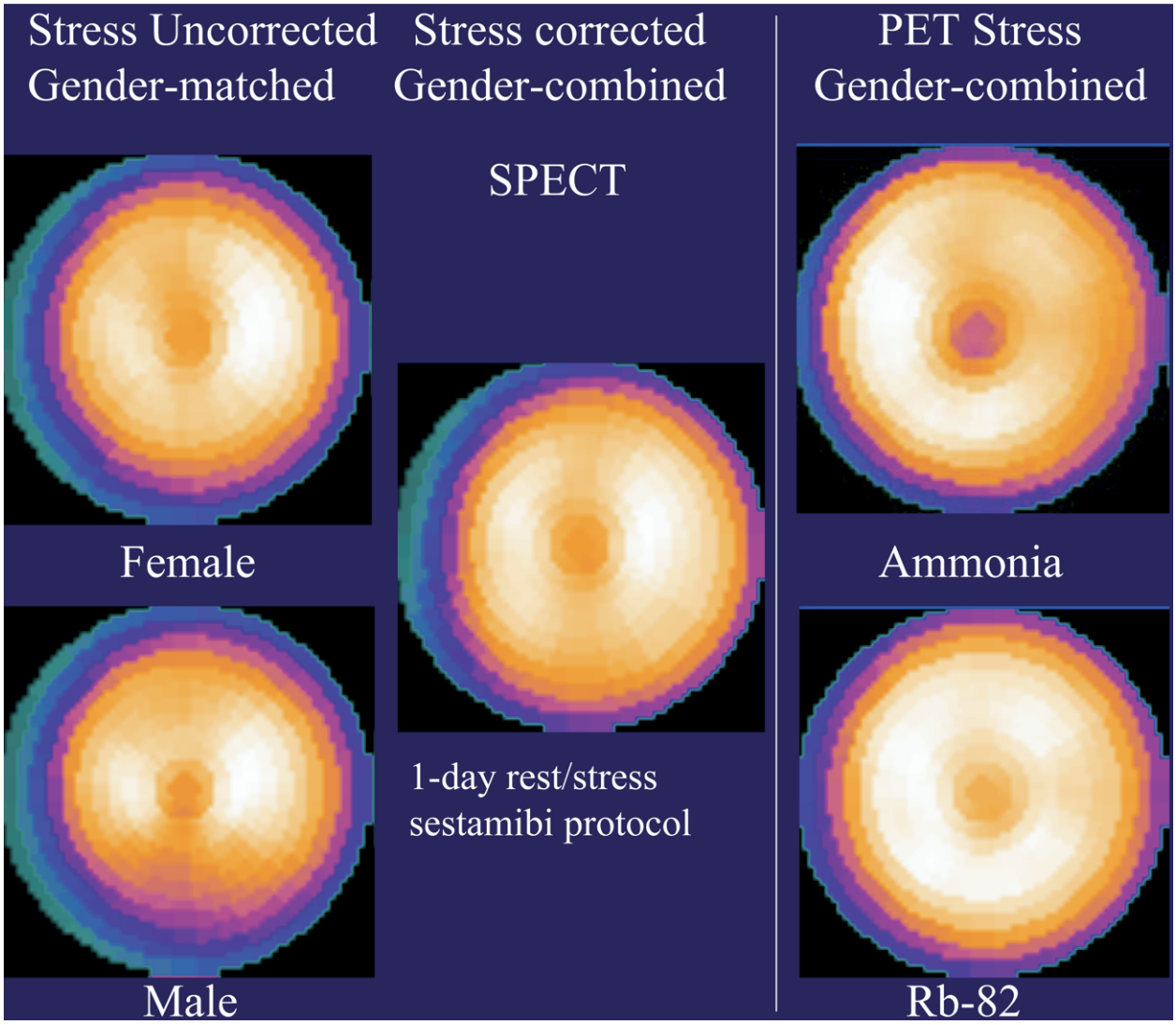

Figure 2. Representative LV normal perfusion distributions. The polar maps represent the mean normal distributions for a stress sestamibi protocol in the *3 left panels* (with and without attenuation correction) and stress N-13 ammonia and Rb-82 distributions. The differences in regional uptake should be noted.

and 150 patients will suffice; otherwise, we use 150 male patients and 150 female patients for a gender-matched normal database.

The 3 described groups are used in the development of the normal database in 3 steps. The first step is to use the low-likelihood group to generate the mean normal 3D distribution and corresponding SDs. Figure 2 illustrates 5 different normal distributions. It should be noted how much the distributions can vary between the different protocols, modalities, and radiopharmaceuticals. The second step is to use the criteria pilot group to calibrate regionally how many SDs below the mean best separate normal from hypoperfused segments. This is done by using experts' interpretation as a calibration standard and then performing receiver operating characteristic analysis to determine the SDs and abnormality extent that best separates the normal from the abnormal group. This determination becomes the criteria for abnormality. It should be noted that although we estimate the summed stress scores as first suggested by Hachamovitch et al,[10] our abnormality criterion is given by the extent of the abnormality as described in Table 1 and not by the summed stress score. The third and final step in establishing a normal database is to use the prospective validation group to characterize the results and to establish the effectiveness of the specific protocol.[11] Table 2 summarizes the existing normal databases for ECTb.

Table 1. Criteria for abnormal perfusion

Hypoperfused defects defined from stress distribution as follows:
Normalized count distribution that falls below the lower limit of normal
Lower limit of normal approximately 2.5 SDs below mean normal (but varies according to actual protocol, gender, attenuation correction)
LV extent ≥3%
Localization to vascular territory
Left anterior descending artery extent ≥10%
Left circumflex artery extent ≥10%
Right coronary artery extent ≥12%
Reversible stress-induced perfusion defects defined from reversibility distribution as follows:
Partial reversibility if region that improves is ≥5% of defect extent
Significant reversibility if region that improves is ≥15% of defect extent

Table 2. Normal databases developed for ECTb

SPECT perfusion normal databases
Enhanced thallium (applicable to both stress/redistribution and stress/reinjection protocols)
Low-dose rest/high-dose exercise stress 1-day sestamibi
Attenuation-corrected low-dose rest/high-dose exercise stress 1-day sestamibi
Low-dose rest/high-dose pharmacologic stress 1-day sestamibi
Attenuation-corrected low-dose rest/high-dose pharmacologic stress 1-day sestamibi
2-Day sestamibi
Low-dose rest/high-dose pharmacologic stress 1-day tetrofosmin
Low-dose stress/high-dose rest 1-day tetrofosmin
Optimized dual isotope (thallium rest/sestamibi stress)
PET perfusion/metabolism normal databases
Rest/stress rubidium (line-source attenuation correction)
Rest/stress rubidium (CT attenuation correction)
Rest/stress N-13 ammonia
Rest rubidium/FDG
Rest ammonia/FDG
Rest enhanced thallium/FDG
High-dose rest sestamibi/FDG
Low-dose rest sestamibi/FDG
Low-dose rest sestamibi with attenuation correction/FDG
High-dose rest tetrofosmin/FDG
Low-dose rest tetrofosmin/FDG
Works in progress
Iodine 123 metaiodobenzylguanidine (*Adreview)
I-123 beta-methyl-iodophenyl-pentadecanoic acid (†Zemiva)
Rest thallium/stress teboroxime

*Adreview manufactured by GE Healthcare, Amersham, UK.
†Zemiva manufactured by Molecular Insight Pharmaceuticals, Boston, Mass.

Measurement of Serial Changes

The database quantification approach described earlier has been shown to be clinically useful in detecting and localizing CAD and in assessing major interventions such as percutaneous coronary intervention or bypass surgery but not for detecting subtle serial changes that might take place with more conservative therapies such as medical therapy or lifestyle changes. To detect these subtle changes, the patient must be used as his or her own control, rather than performing a comparison to normal databases over time. By performing alignment of the 3D myocardial perfusion distribution, Faber et al[12] have shown that we can detect 10% or greater differences in serial perfusion studies in single patients.

QUANTIFICATION OF MYOCARDIAL FUNCTION

Myocardial Thickening

All measurements of LV function in ECTb are based on our ability to measure myocardial thickening throughout the cardiac cycle. In 1990 Galt et al[13] from our group showed that as a result of the limited spatial resolution of our imaging cameras compared with the myocardial thickness, partial-volume effects cause an almost linear change in maximal counts in myocardial segments as a change in thickness. Thus we determined that thickening could be measured for a myocardial segment as a change in maximal counts for that segment throughout the cardiac cycle. Our approach uses the myocardial location of the maximal count (corrected for scatter) to determine the midpoint of the myocardial wall segment. The assumption is made that at end diastole, the LV myocardial thickness is 1 cm thick (ie, 5 mm on either side of the midpoint). This defines both the 3D endocardial and epicardial surfaces. It then uses the regional change in counts from the end-diastolic frame to determine the change in endocardial/epicardial surface location. For example, if at end systole, the myocardial counts in a segment double, the thickness will also double from 1 to 2 cm.

Global Function

From these endocardial surfaces, LV volumes are determined in terms of the total number of voxels

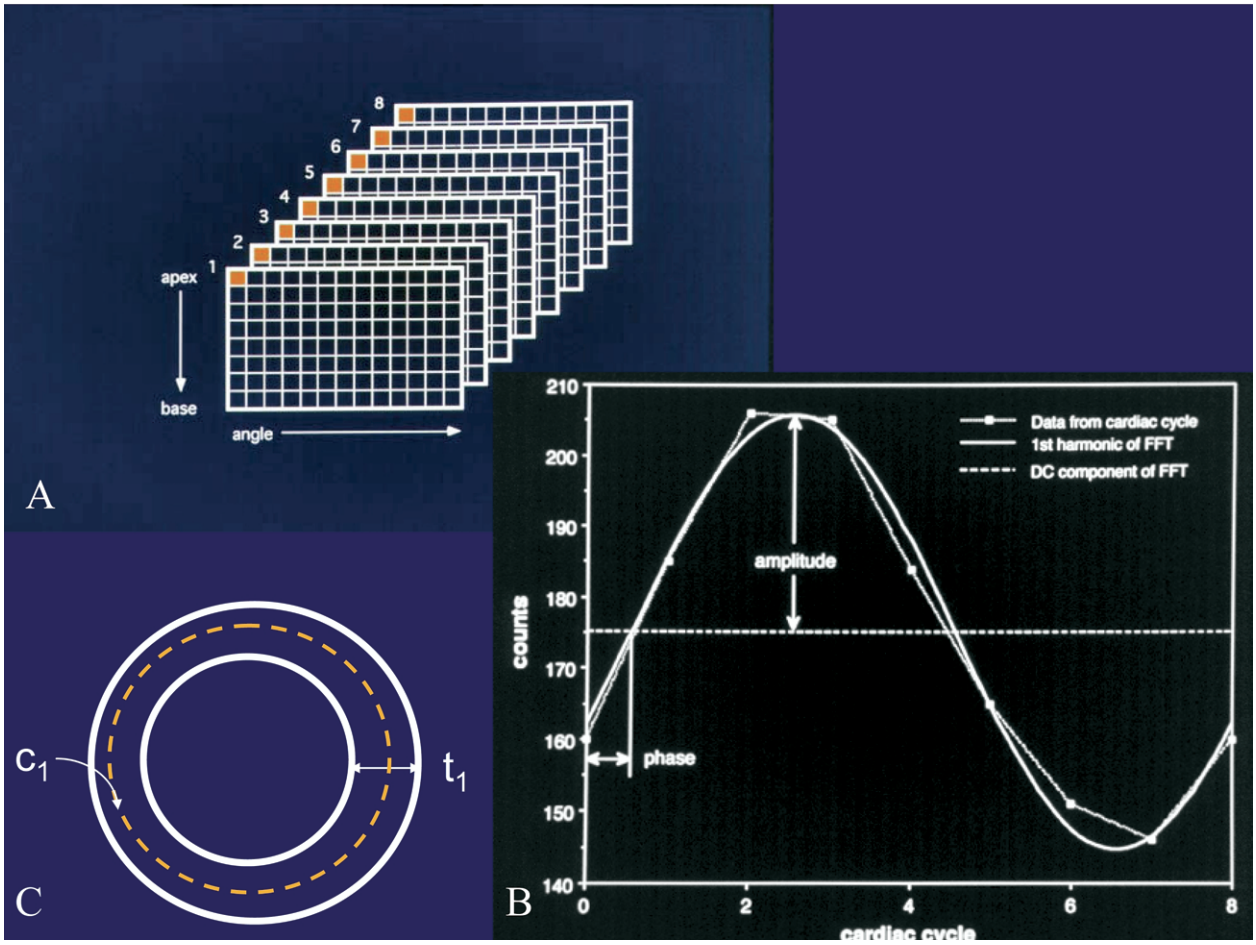

Figure 3. ECTb method of extracting regional thickening and OMC (phase) via Fourier analysis. **A** depicts how each of 8 3D count distributions is extracted from the 8 reconstructed electrocardiography-gated LV frames. Each matrix represents the maximal count samples from the apex to the base (*rows*) for each angular sample (*columns*). **B** shows how a single 8-sample maximal count thickening curve is fitted to a first-harmonic Fourier component to replace it with a continuous curve. **C** illustrates how the 3D endocardial and epicardial boundaries are modeled by starting with the maximal count samples in the middle of the left ventricle, assuming a 1-cm thickness at end diastole (5 mm to either side of the maximum counts), and then varying the thickness as a function of the change in counts given by the thickening curve. At the end of this process, 3D endocardial and epicardial LV boundaries are generated, which are used to calculate volumes, ejection fraction, and LV mass.

(volume elements) inside the surface. The largest cavity volume throughout the cardiac cycle is defined as the end-diastolic volume (EDV), the smallest cavity volume is defined as the end-systolic volume (ESV), and LV ejection fraction is calculated as the stroke volume (EDV minus ESV) divided by the EDV. The volume between the epicardial and endocardial 3D surfaces yields the LV myocardial volume, which—when multiplied by the specific gravity of water—estimates the myocardial mass. Because the LV mass is conserved over the cardiac cycle, we report the average mass as a more accurate determination.

One important aspect of our approach is that it was designed to provide accurate temporal sampling via 8 frames per cardiac cycle, as shown by Cooke et al.[14] This was done by use of Fourier analysis of the phase and amplitude of the maximal count variation in each 3D myocardial segment. Thus, if conventional temporal sampling is used, 8 frames are not enough to accurately define either global or regional end diastole or end systole; the Fourier analysis approach replaces this discrete curve by a continuous curve on point-by-point bases (Figure 3). This has the effect of providing a much higher temporal resolution. Another important aspect of our approach is that we integrated this functional analysis with the quantification of myocardial perfusion as reported by Faber et al.[15]

Table 3. Criteria for normal LV global function

Ejection fraction ≥51%
EDV <171 mL
ESV <70 mL

Clinically Validated Functional Measurements

The accuracy of how well each method determines global and regional parameters of LV function depends on a number of variables. The main variables are the accuracy of the following: the definition of the endocardial and epicardial 3D surfaces, the valve plane, and the temporal, spatial, and contrast resolution. These main variables are also affected by a number of acquisition, processing, and patient-dependent variables. The accuracy of our LV ejection fraction calculations has been established by comparison to echocardiography[16] and magnetic resonance imaging[17] and against other electrocardiography-gated MPI techniques.[17,18] The lower limits of normal function are shown in Table 3.

Phase Analysis to Measure LV Dyssynchrony

Chen et al[19] have reported how we quantify LV dyssynchrony as the regional time delays in the onset of mechanical contraction (OMC) over the LV myocardium. By use of the Fourier analysis explained earlier (and in Figure 3), the 3D count distributions are extracted from each of the 8 LV short-axis data sets to extract a phase array (3D regional phases). The calculated phase array describes the regional OMC of the myocardium in 3 dimensions, with 0° corresponding to the peak of the R wave and one R-R interval corresponding to 360° (Figure 4). The following 5 quantitative indices were calculated from each phase array: peak phase, which is the most frequent phase (the phase corresponding to the peak of the phase histogram); phase SD (ie, the SD of the phase distribution); phase histogram bandwidth (ie, the width of the band), which includes 95% of the elements in the phase distribution; phase histogram skewness (ie, the skewness of the phase histogram), which indicates the symmetry of the histogram (where positive skewness indicates the histogram is skewed to the right with a longer tail to the right of the peak phase); and phase histogram kurtosis (ie, kurtosis of the phase histogram), which indicates the degree to which the histogram is peaked (where a histogram with a higher peak within a narrower band has higher kurtosis). The lower limits of normal OMC are shown in Table 4. Henneman et al[20] have validated our approach using echocardiography tissue Doppler imaging as a gold standard.

PET TOOLS FOR QUANTITATIVE ANALYSIS

Quantification of myocardial perfusion of PET tracers uses the same database quantification approach explained earlier except that the normal limits are generated by use of PET radiopharmaceuticals. Normal patterns are shown in Figure 2 for rubidium 82 and nitrogen 13 ammonia, and the PET normal databases are listed in Table 2. These have been validated clinically including the latest Rb-82 PET/computed tomography (CT) protocol.[21]

To quantify the perfusion/metabolism match/mismatch pattern as a marker of hibernation, 4 quantitative tools have been implemented in ECTb. One of these tools is based on the fluorodeoxyglucose (FDG) study alone, whereas the other three tools assess the extent of match/mismatch defects between defects seen with FDG (metabolism) and Rb-82 (perfusion), by use of the Rb-82 normal database for comparison.[22] The optimal thresholds for detecting mismatch by use of these tools have been determined by Santana et al[22] as the values with the best prognostic stratification of patients with ischemic cardiomyopathy undergoing myocardial viability assessment.

PET Tool Using Only FDG Uptake

This tool adapts to FDG, the traditional approach for quantifying myocardial viability, by use of the resting myocardial perfusion tracer distribution (Rb-82, N-13 ammonia, Tl-201, Tc-99m sestamibi, and Tc-99m tetrofosmin). The FDG-alone tool calculates the extent of the nonviable and viable myocardium by use of a user-defined threshold of the maximum LV myocardium FDG counts. For this research, the extent of LV myocardium that was below the 50% threshold was considered nonviable. Therefore the percentage of the myocardium with uptake greater than 50% was considered viable.

PET Tools Using FDG Distribution Normalized to a Perfusion Database

These results are in relation to an automatic quantitative program applied to the resting perfusion study. The hypoperfused areas can be identified by use of a normal database; the remaining normal areas are then used for normalization. The average count value in the entire extent of normally perfused regions is computed for both the perfusion and FDG studies, and then the FDG is scaled so that its average value in the normal region is equal to that in the perfusion study. After normalization, 2 approaches are used to define areas of mismatch (Figure 5). In the first approach, the normalized perfusion distribution is subtracted from the normalized me-

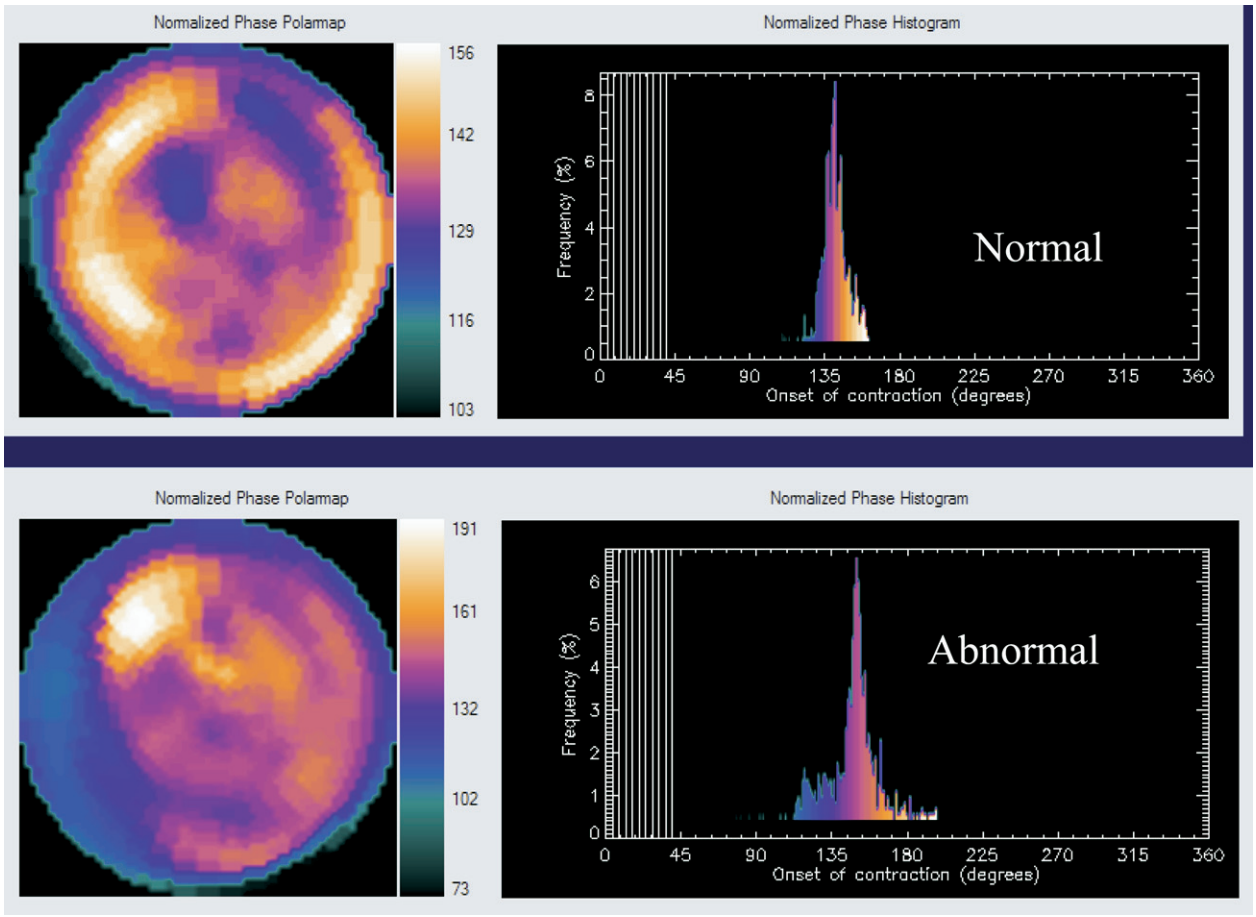

Figure 4. Examples of OMC phase distributions in patients with normal (*top*) and abnormal (*bottom*) LV synchrony. The polar maps depict the regional phase of OMC, where the darker colors illustrate where the wave of propagation starts and the brighter colors show where it ends. The phase histograms are color-coded to the phase polar maps and plot the number of voxels (frequency) with a particular phase (OMC). The abnormal patient (*bottom*) is the same patient as in Figure 1. It should be noted how this patient exhibits a broader (more dyssynchronous) distribution than the normal patient and how the hypoperfused region is the last to contract.

tabolism distribution. The difference between the distributions is expressed as a percentage of the normalized metabolism distribution. A threshold for this percent difference can be set at any level. In the low-flow match/mismatch approach, regions in the distribution that are above the threshold, and that also have abnormal perfusion, are those that have relatively increased metabolism coexistent with relatively decreased perfusion (ie, a mismatch) (Figure 5*A*).

In the all-flow mismatch approach (Figure 5*B*), all areas that exhibit increased FDG uptake above the user-set threshold, instead of just those areas that have abnormal resting perfusion (low-flow mismatch) (Figure 5*A*), are defined as mismatch.

A second approach using both the perfusion and FDG distributions is to apply a set threshold to the metabolism distribution itself. Regions above the threshold are considered either to be relatively normal or to correspond to increased areas of metabolism. Any area above the threshold that is also abnormal for perfusion can be considered a mismatch consistent with myocardial hibernation.

THREE-DIMENSIONAL DISPLAYS AND IMAGE FUSION

Three-Dimensional Displays

We use 3D graphics techniques to overlay results of perfusion quantification onto a representation of a specific patient's left ventricle. This representation is generated by use of endocardial or epicardial surface points extracted from the perfusion data. Our approach for detecting the surface of the myocardium starts with the

Table 4. Normal limits of OMC phases

	Range	Mean	SD
Peak phase (°)			
Male	96-161	134.5	14.3
Female	107-167	140.2	14.9
Phase SD (°)			
Male	6.3-27.6	14.2	5.1
Female	5.1-31.4	11.8	5.2
Histogram bandwidth (°)			
Male	22-81	38.7	11.8
Female	18-62	30.6	9.6
Histogram skewness			
Male	2.84-5.95	4.19	0.68
Female	3.05-6.10	4.60	0.72
Histogram kurtosis			
Male	8.45-45.32	19.72	7.68
Female	9.65-48.19	23.21	8.16

3D coordinates of the maximal myocardial count samples created during perfusion quantification.[23] The coordinates of each sampled point are filtered to remove noise. By assuming that the myocardium is 1 cm thick at end diastole, an estimate of the endocardial surface can be generated by subtracting a distance of 5 mm from the myocardial center point. Adding 5 mm estimates the epicardial surface. We have shown that this modeling of the epicardial surface from MPI studies agrees favorably with magnetic resonance imaging endocardial surfaces.[24]

Once extracted, boundary points can be connected into triangles or quadrilaterals, which are in turn connected into a polygonal surface representing the endocardial or epicardial surface. Once a surface is generated, perfusion is displayed by assigning to each triangle or quadrilateral a color corresponding to the counts extracted from the myocardium at that sample during a quantification process. Colors can be interpolated between triangles to produce a continuum of colors across the myocardium, or the triangles can be left as patches of distinct color. Figure 1 shows the relationship between a polar map representation of the LV myocardial perfusion and a 3D representation.

In general, 3D displays have the advantage over polar maps of showing the actual size and shape of the left ventricle, as well as the extent and location of any defect in a very realistic manner. Our studies have demonstrated that such 3D displays are better or at least equivalent for estimating the size and location of defects than either polar maps or the original slice-by-slice displays.[25] The greatest disadvantage of 3D displays is that they require more computer screen space (and therefore more film or paper for hard copies) than polar maps. The entire left ventricle can be visualized in a single circular polar map, but only one side of the left ventricle can be seen when it is displayed by use of 3D graphics.

Heartfusion

Often, more than one type of imaging procedure is used to evaluate patients for cardiac disease. Coronary angiography and CT coronary angiography (CTCA) are used for diagnosis of coronary artery stenosis; SPECT and PET are used to evaluate myocardial perfusion. There are major advantages in automatically reorienting and rescaling multimodality images so that they are in the same position and orientation as each other, as well as in displaying their information in a unified manner. This process is termed multimodality registration, fusion, or unification. Although physicians frequently perform this image integration mentally, automating the processes may improve their ability to assimilate the large amount of data and to draw meaningful conclusions from the data. After automatic unification, comparisons between information contained in the studies are straightforward, as cardiac structures can be viewed in the same orientation or sliced in the same manner. Cause-and-effect relationships may be more apparent, and anatomy and physiology may be more easily compared.

Ideally, accurate assessment of the extent and severity of CAD requires the integration of physiologic information derived from SPECT (or PET) perfusion images and anatomic information derived from coronary angiography or CTCA. This integration has been performed by registering a 3D LV model representing myocardial perfusion with the patient's own 3D coronary artery tree and presenting both in a single unified display. The patient-specific coronary artery tree is obtained from a 3D geometric reconstruction performed on simultaneously acquired, digital, biplane angiographic projections or from CTCA obtained from a 16-slice (or greater) CT scanner. The 3D reconstructed arterial tree is approximated by successive conical segments and is scaled and rotated to fit onto the myocardial surface. The left or right coronary arteries are registered with the myocardial perfusion surface model by automatically minimizing a cost function that describes the relationships of the coronary artery tree with the interventricular and atrioventricular groove and the surface of the myocardium. Figure 6 illustrates this unified display.

Faber et al[26] validated this Heartfusion (Syntermed, Inc) tool in a unique group of patients with single-vessel disease who were given Tc-99m tetrofosmin while undergoing angioplasty. This report showed that the physiologic mass at risk from the SPECT study corresponded favorably with the fused anatomic mass at risk from the

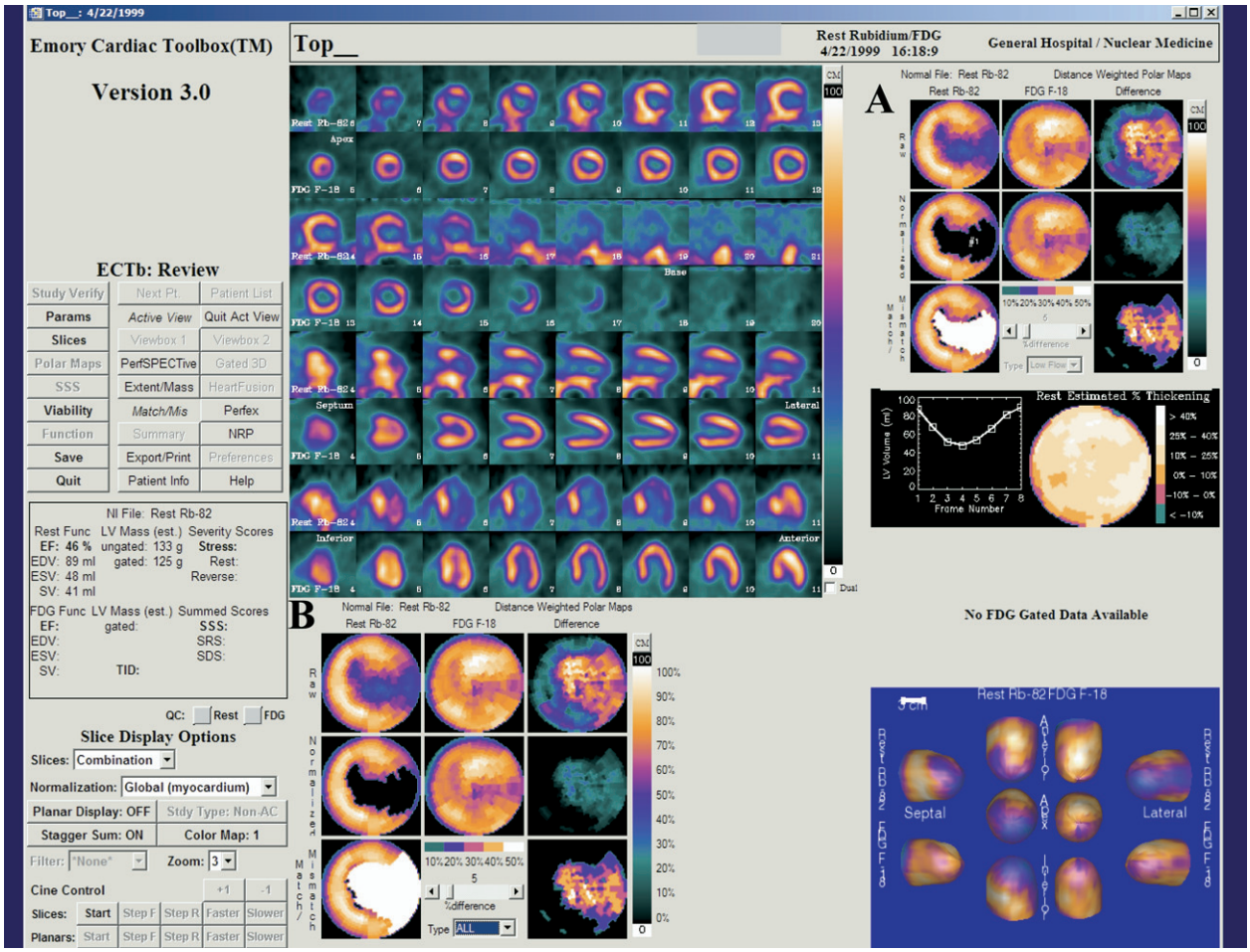

Figure 5. Quantitative perfusion/metabolism match/mismatch results. The oblique slices in this patient depict a resting Rb-82 perfusion distribution with a hypoperfused lateral wall (*alternating top rows*) with a normal FDG metabolic distribution (*alternating bottom rows*). **A** (*top right*) shows how the resting hypoperfused region highlighted in black improves significantly (*filled in white*) by more than 5% by use of the low-flow approach, where only the hypoperfused region is considered. **B** shows results via the all-flow approach, the algorithm where all regions that improve by 5% are considered regardless of whether they were found to be quantitatively hypoperfused.

coronary arteriography as it should in this single-vessel disease population. More recently, Santana et al[27] showed how using our fusion of the MPI plus CTCA 3D distributions resulted in a higher accuracy of diagnosing CAD when compared with the independent MPI and CTCA information. Rispler at al[28] have convincingly shown that our fusion algorithm increased the specificity of detecting CAD with CTCA from 63% to 95%.

PERFEX: Perfusion Expert System

Expert systems are becoming popular because they are designed to circumvent the problem of having few experts in areas where many are needed. Thus expert systems attempt to capture the knowledge or expertise of the human domain expert and provide it to a large number of non-experts. We have developed PERFEX (Syntermed, Inc) to assist in diagnosing CAD from SPECT and PET MPI studies.[29] This type of approach has the potential for standardizing the image interpretation process. After reviewing 291 studies from patients with angiographically documented CAD, heuristic rules were derived that best correlated the presence and location of perfusion defects on Tl-201 SPECT studies with coronary lesions. These rules operate on data that are input to the expert system from the ECTb quantification process, which identifies defects as portions of the myocardium where normalized perfusion falls below a predetermined number of SDs when compared with a gender-matched normal file and identifies reversibility as defects at stress that improve at rest. An automatic feature extraction program then describes the location

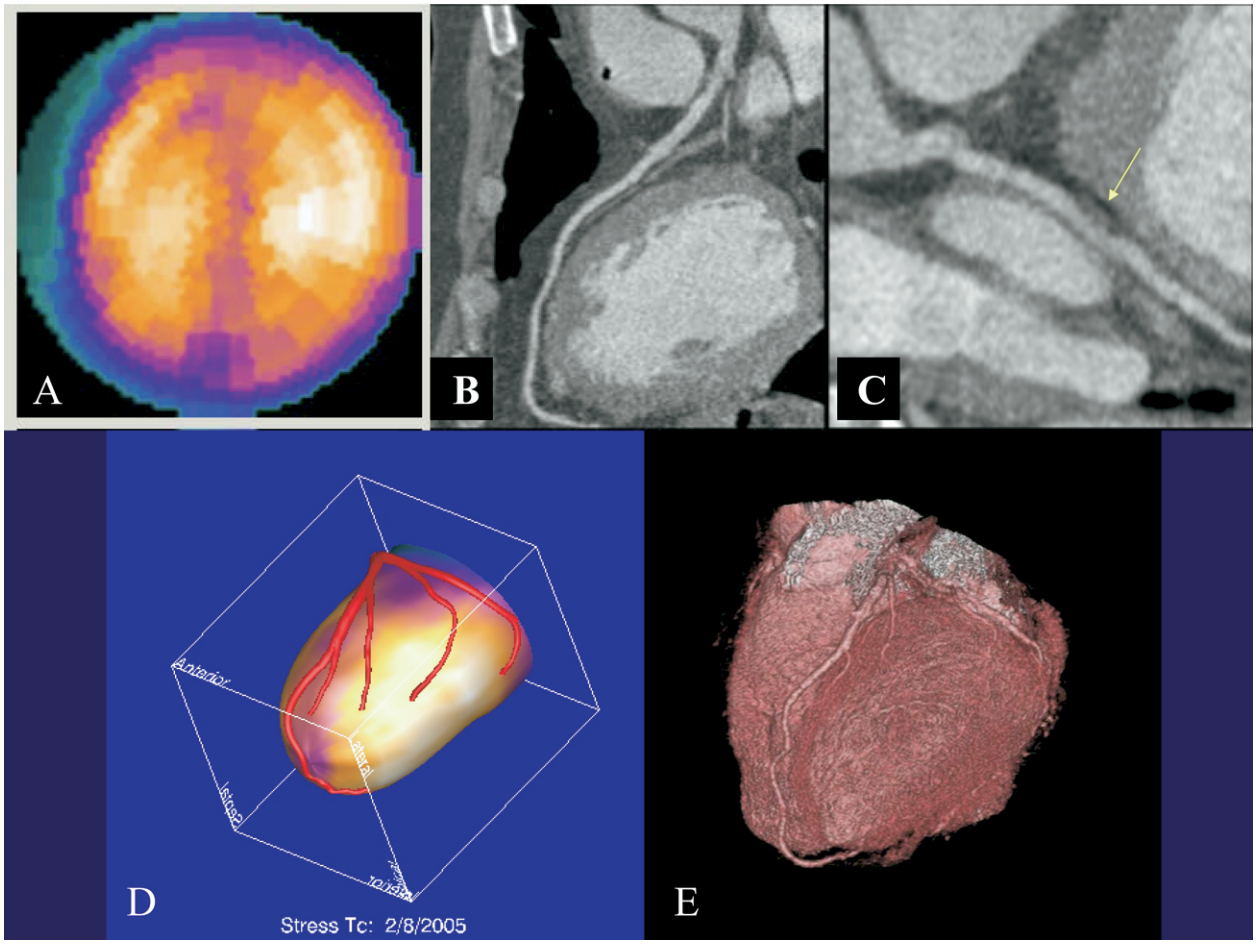

Figure 6. Example of how image fusion improves specificity of myocardial perfusion (MPI) and CTCA. **A** shows a stress perfusion polar map with questionable anterior and inferior reduction in counts. **B** shows a normal left anterior descending artery from the CTCA study. **C** shows a 30% soft plaque in the first obtuse marginal (arrow). **D** illustrates the fused MPI + CTCA display, where the vessel in question is perfusing the most normal myocardial region. Because the MPI questionable area and the CTCA questionable area do not coincide in the fused display, the study was interpreted as normal. **E** shows the CTCA 3D surface representation for comparison.

and severity of each defect or reversibility. The location is expressed in the form of 32 possible descriptors and is defined as coordinates of both depth (basal, medial, distal-apical, and proximal-apical) and angular location (8 subsets of the septal, inferior, lateral, and anterior myocardial walls). The severity is expressed in terms of certainty factors, which range from −1 to +1 (where −1 means there is definitely no disease, +1 means there is definitely disease, and the range from −0.2 to +0.2 means equivocal or indeterminable). By use of the aforementioned features, the expert system automatically determines the location, size, and shape of each defect/reversibility. This information is used to "fire" or execute the 253 heuristic rules to produce new facts or to draw new inferences. For each input parameter and for each rule, a certainty factor is assigned, which is used to determine the certainty of the identification and location of a coronary lesion. The results of the expert system interpretation for the patient in Figure 1 are shown in Figure 7, which correctly identified ischemic left anterior descending artery disease.

PERFEX has undergone extensive validation in 655 prospective patients.[29] This study showed that the diagnostic performance of PERFEX for interpreting myocardial perfusion SPECT studies is comparable to that of nuclear experts in detecting and locating CAD.

SUMMARY

The inherently digital nuclear cardiology images coupled with the tremendous advances in computer hardware and software have facilitated our progress in

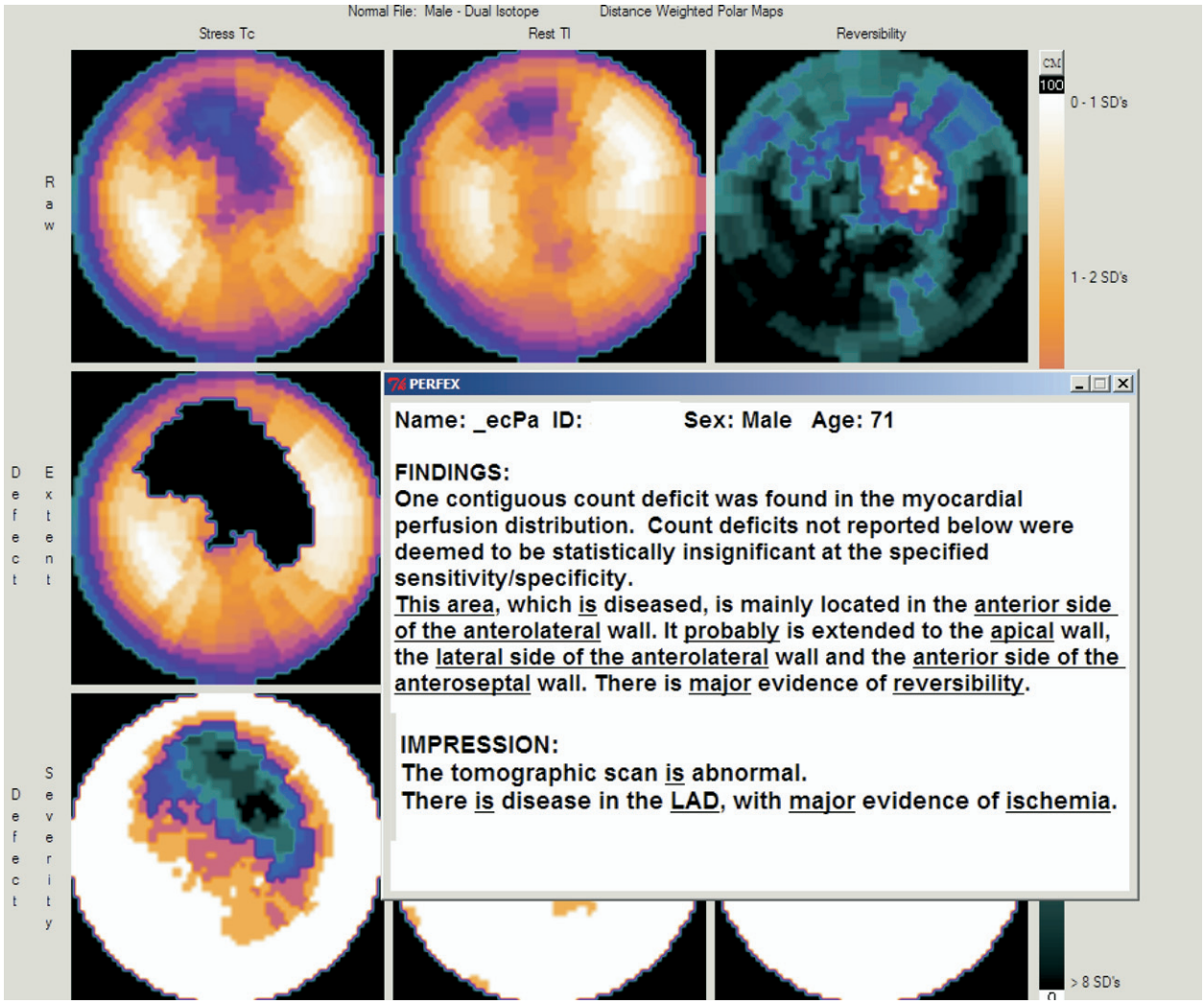

Figure 7. Conclusion reached by the PERFEX expert system for the patient study from Figure 1. PERFEX provides decision support by suggesting the study findings and impression. Each conclusion is underlined in the dialogue. By clicking on each underlined word, PERFEX provides justification for the conclusion reached.

total automatic analysis; multidimensional, multimodality display; quantification of all clinically relevant parameters; and computer-assisted decision support. Our Emory team has created ECTb as a pipeline to take advantage of this modern technology to bring to nuclear cardiology practitioners clinically validated tools to visualize and quantify myocardial perfusion, function, and metabolism from electrocardiography-gated myocardial SPECT and PET studies.

Acknowledgment

The research that generated the science implemented in ECTb was funded in part by National Institutes of Health grants HL070422, HL068904, HL42052, and LM06726. Some of the authors receive royalties from the sale of ECTb (E.V.G., T.L.F., C.D.C., and R.D.F.) related to the research described in this article. The terms of this arrangement have been reviewed and approved by Emory University in accordance with its conflict-of-interest practice.

References

1. Garcia EV, Van Train K, Maddahi J, Prigent F, Friedman J, Areeda J, et al. Quantification of rotational thallium-201 myocardial tomography. J Nucl Med 1985;26:17-26.
2. Garcia EV, DePuey EG, DePasquale EE. Quantitative planar and tomographic thallium-201 myocardial perfusion imaging. Cardiovasc Intervent Radiol 1987;10:374-83.
3. DePasquale E, Nody A, DePuey G, Garcia E, Pilcher G, Bredleau C, et al. Quantitative rotational thallium-201 tomography for identifying and localizing coronary artery disease. Circulation 1988;77:316-27.

4. DePuey EG, Roubin GS, DePasquale EE, Nody AC, Garcia EV, King SB, et al. Sequential multivessel coronary angioplasty assessed by thallium-201 tomography. Cathet Cardiovasc Diagn 1989;18:213-21.
5. Klein JL, Garcia EV, DePuey EG, Cambell J, Taylor AT, Pettigrew RI, et al. Reversibility bullseye: a new polar bull's-eye map to quantify reversibility of stress induced SPECT Tl-201 myocardial perfusion defects. J Nucl Med 1990;31:1240-6.
6. Garcia E, DePuey EG, Sonnemaker RE, Neely HR, DePasquale EE, Robbins WL, et al. Quantification of the reversibility of stress induced SPECT thallium-201 myocardial perfusion defects: a multicenter trial using bull's-eye polar maps and standard normal limits. J Nucl Med 1990;31:1761-5.
7. Gibbons RJ, Miller TD, Christian T. Infarct size measured by single photon emission computed tomographic imaging with ^{99m}Tc-sestamibi: a measure of the efficacy of therapy in acute myocardial infarction. Circulation 2000;101:101-8.
8. Van Train KF, Areeda J, Garcia EV, Cooke CD, Maddahi J, Kiat H, et al. Quantitative same-day rest-stress technetium-99m-sestamibi SPECT: definition and validation of stress normal limits and criteria for abnormality. J Nucl Med 1993;34:1494-502.
9. Grossman GB, Garcia EV, Bateman TM, Heller GV, Johnson LL, Folks RD, et al. Quantitative Tc-99m sestamibi attenuation-corrected SPECT: development and multicenter trial validation of myocardial perfusion stress gender-independent normal database in an obese population. J Nucl Cardiol 2004;11:263-72.
10. Hachamovitch R, Berman DS, Kiat H, Cohen I, Cabico JA, Friedman J, et al. Exercise myocardial perfusion SPECT in patients without known coronary artery disease: incremental prognostic value and use in risk stratification. Circulation 1996;93:905-14.
11. Van Train KF, Garcia EV, Maddahi J, Areeda J, Cooke CD, Kiat H, et al. Multicenter trial validation for quantitative analysis of same-day rest-stress technetium-99m-sestamibi myocardial tomograms. J Nucl Med 1994;35:609-18.
12. Faber TL, Modersitzki J, Folks RD. Garcia EV. Detecting changes in serial myocardial perfusion SPECT: a simulation study. J Nucl Cardiol 2005;12:302-10.
13. Galt JR, Garcia EV, Robbins W. Effects of myocardial wall thickness on SPECT quantification. IEEE Trans Med Imaging 1990;9:144-50.
14. Cooke CD, Garcia EV, Cullom SJ, Faber TL, Pettigrew RI. Determining the accuracy of calculating systolic wall thickening using a fast Fourier transform approximation: a simulation study based on canine and patient data. J Nucl Med 1994;35:1185-92.
15. Faber TL, Cooke CD, Folks RD, Vansant JP, Nichols KJ, DePuey EG, et al. Left ventricular function and perfusion from gated SPECT perfusion images: an integrated method. J Nucl Med 1999;40:650-9.
16. Nichols K, Lefkowitz D, Faber T, Folks R, Cooke D, Garcia EV, et al. Echocardiographic validation of gated SPECT ventricular function measurements. J Nucl Med 2000;41:1308-14.
17. Faber TL, Vansant JP, Pettigrew RI, Galt JR, Blais M, Chatzimavroudis G, et al. Evaluation of left ventricular endocardial volumes and ejection fractions computed from gated perfusion SPECT with MR: comparison of two methods. J Nucl Cardiol 2001;8:645-51.
18. Nichols K, Santana CA, Folks R, Krawczynska E, Cooke CD, Faber TL, et al. Comparison between ECTb and QGS for assessment of left ventricular function from gated myocardial perfusion SPECT. J Nucl Cardiol 2002;9:285-93.
19. Chen J, Garcia EV, Folks RD, Cooke CD, Faber TL, Tauxe EL, et al. Onset of left ventricular mechanical contraction as determined by phase analysis of ECG-gated myocardial perfusion SPECT imaging: development of a diagnostic tool for assessment of cardiac mechanical dyssynchrony. J Nucl Cardiol 2005;12:687-95.
20. Henneman MM, Chen J, Ypenburg C, Dibbets P, Bleeker GB, Boersma E, et al. Phase analysis of gated myocardial perfusion single-photon emission computed tomography compared with tissue Doppler imaging for the assessment of left ventricular dyssynchrony. J Am Coll Cardiol 2007;49:1708-14.
21. Santana CA, Folks RD, Garcia EV, Verdes L, Hainer J, Di Carli MF, et al. Quantitative Rb-82 PET/CT: development and validation of myocardial perfusion database. J Nucl Cardiol 2007;48:1-7.
22. Santana CA, Folks RD, Faber TL, Verdes L, Narla R, Cooke D, et al. Value of quantitative PET tools for prognostic stratification of patients with ischemic cardiomyopathy undergoing myocardial viability assessment [abstract]. J Nucl Med 2005;46:264P.
23. Garcia EV, Cooke CD, Van Train K, Folks RD, Peifer JW, DePuey EG, et al. Technical aspects of myocardial SPECT imaging with Tc-99m sestamibi. Am J Cardiol 1990;66:23E-31E.
24. Faber TL, Cooke CD, Peifer JW, Pettigrew RI, Vansant JP, Leyendecker JR, et al. Three-dimensional displays of left ventricular epicardial surface from standard cardiac SPECT perfusion quantification techniques. J Nucl Med 1995;36:697-703
25. Cooke CD, Vansant JP, Krawczynska EG, Faber TL, Garcia EV. Clinical validation of three-dimensional color-modulated displays of myocardial perfusion. J Nucl Cardiol 1997;4:108-16.
26. Faber TL, Santana CA, Garcia EV, Candell-Riera J, Folks RD, Peifer JW, et al. Three-dimensional fusion of coronary arteries with myocardial perfusion distributions: clinical validation. J Nucl Med 2004;45:745-53.
27. Santana CA, Garcia EV, Faber TL, Esteves F, Halkar R, Ornelas M, et al. Performance of myocardial perfusion (MPI), MPI plus CT coronary angiography (MPI+CTA) and the 3D fusion of MPI and CTA (MPI/CTA Fusion) in the diagnosis of CAD [abstract]. J Nucl Med 2007;48(Suppl 2):232P.
28. Rispler S, Keidar Z, Ghersin E, Roguin A, Soil A, Dragu R, et al. Integrated single-photon emission computed tomography and computed tomography coronary angiography for the assessment of hemodynamically significant coronary artery lesions. J Am Coll Cardiol 2007;49:1059-67.
29. Garcia EV, Cooke CD, Folks RD, Santana CA, Krawczynska EG, De Braal L, et al. Diagnostic performance of an expert system for the interpretation of myocardial perfusion SPECT studies. J Nucl Med 2001;42:1185-91.